NAVORD REPORT 2710
FIRST REVISION

ON THE OBLIQUE REFLECTION OF UNDERWATER SHOCKWAVES FROM A FREE SURFACE I

1 NOVEMBER 1956

U. S. NAVAL ORDNANCE LABORATORY
WHITE OAK, MARYLAND

NAVORD Report 2710

ON THE OBLIQUE REFLECTION OF UNDERWATER SHOCKWAVES FROM A FREE SURFACE I

by:

J. H. Rosenbaum and H. G. Snay

Approved by: E. Swift, Jr.
Chief, Explosion Hydrodynamics Division

ABSTRACT: On the basis of Penney's and Keil's quasi-stationary theory of oblique shock reflection, an approximate theory of the anomalous reflection phenomenon is derived. This theory permits the determination of peak pressure, shape and duration of the positive pressure pulse and appears to be applicable to shallow explosions in deep water at depths greater than 3 charge radii from the free surface.

U. S. Naval Ordnance Laboratory
White Oak, Silver Spring, Maryland

NAVORD Report 2710 1 November 1956

The study reported here was carried out under Task Re2c-65-1 as part of a program aimed at investigating the anomalous surface reflection of shockwaves from shallow explosions in deep water. Since the material in this report is of immediate interest to other groups, it is published in its present form at this time. The experimental data with which this work can be compared will be reported later.

The authors wish to point out the essentially non-stationary nature of the entire problem, and the serious assumptions inherent in the stationary flow simplification used in this paper. The senior author (H. G. S.) has suggested a possible attack leading to a more exact solution, which will be presented later if time permits.

This report is for information only, and the opinions expressed herein are those of the authors.

This revision supersedes NAVORD Report 2710, dated 1 January 1953.

W. W. WILBOURNE
Captain, USN

J. E. Ablard
By direction

TABLE OF CONTENTS

NAVORD Report 2710

ON THE OBLIQUE REFLECTION OF UNDERWATER SHOCKWAVES FROM A FREE SURFACE I

I INTRODUCTION

When a shockwave produced by an underwater explosion comes in contact with a free surface, its pressure must drop to approximately atmospheric, or more precisely, to the same pressure as the air shock produced at the interface. As a result, a tension wave is reflected from the surface, which modifies the incident wave in the water. At the free surface, the situation of oblique reflection of a shockwave can be treated as a quasi-stationary flow problem, where the pressure is relieved by a flow around a Prandtl-Meyer corner [L]*. As was first pointed out by Penney, the flow into the expansion wedge becomes subsonic if the glancing angle of the shockwave is sufficiently small. As a result, the rarefaction wave overtakes the incident shock front and attenuates it. This leads to a region of peak pressure distortion, whose boundaries have been calculated by Penney and Keil [I] for a spherical shockwave.

In the present paper, an attempt is made to analyze the phenomenon within the distorted region. A pseudo-stationary approach is used, and as a result it appears that the pressure relief in this region takes place in two stages: Part of the pressure is released by means of a wave which is traveling faster than the incident shock; the remaining pressure is then relieved through a Prandtl-Meyer corner flow. On the basis of this treatment, it is possible to construct pressure-time histories for shockwaves in the regions of anomalous reflection.

---

*All such letters refer to the list of references at the end of this report.

II REGULAR REFLECTION AND THE PRANDTL-MEYER CORNER FLOW

The interaction of a plane shockwave of infinite duration with a free surface at a sufficiently large glancing angle, can be represented by a stationary flow pattern if a steady flow is superposed parallel to the surface. This flow is shown by the vector - U sec Θ in Figure 1, where U is the propagation velocity of the shockwave, and Θ is the angle between the wave front and the normal to the surface. Since a positive disturbance of finite amplitude must travel with supersonic velocity ($U > c_o$, the sound velocity in the undisturbed medium), this superposed flow is always supersonic. This flow corresponds to the undisturbed water before the shock front, as observed from the moving point of intersection of the shock front with the free surface. The flow behind the shock front is modified by a quantity u, the actual particle velocity behind the front. This flow, f_1, can be obtained by vector addition of the original superposed flow and u, as shown at the bottom of Figure 1.

The pressure at the free water surface must remain atmospheric. As long as the flow f_1 is supersonic (or sonic), this condition can be realized by a stationary expansion wave, centered at the point of intersection of the shock front with the surface. This is the well-known Prandtl-Meyer corner flow. Figure 2 illustrates this flow more clearly; the expansion wedge consists of the Mach lines of the corner flow.

According to the Prandtl-Meyer analysis of a 2-dimensional irrotational steady supersonic expansive flow around a corner [L], the relationship between the angular deflection of

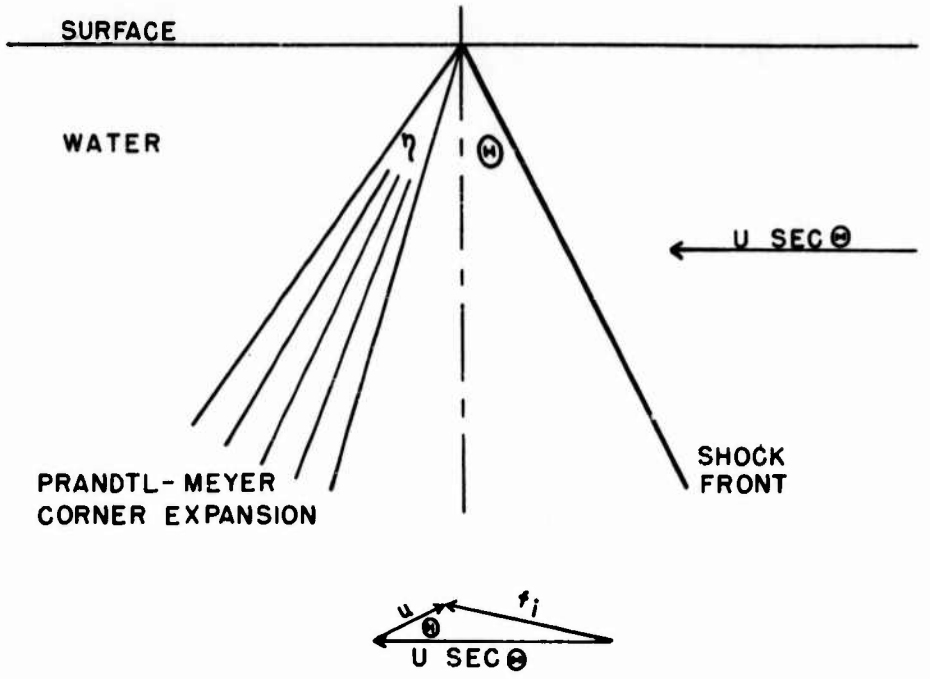

FIG. 1 REGULAR REFLECTION OF PLANE SHOCKWAVE

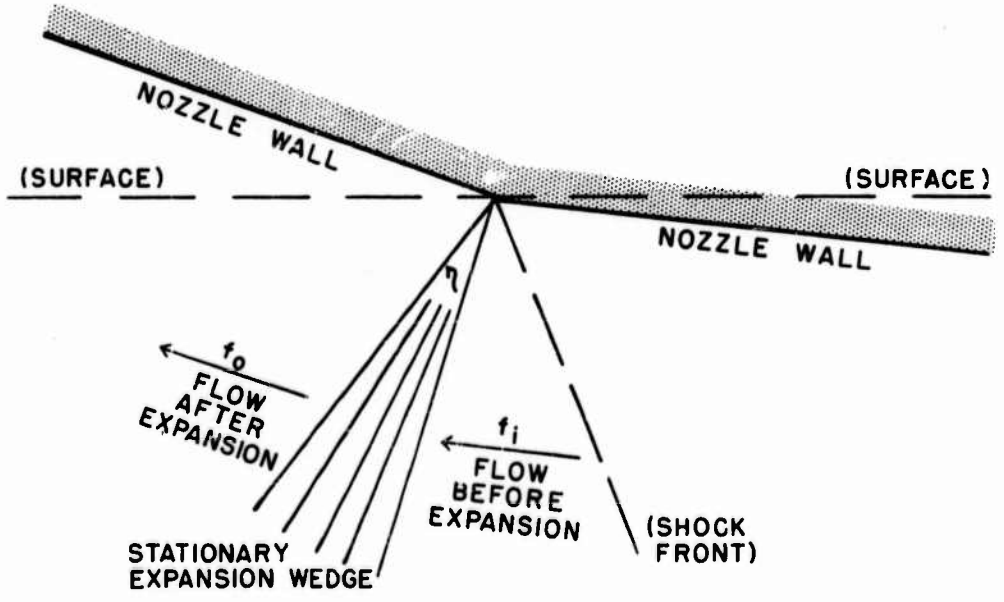

FIG. 2 PRANDTL-MEYER CORNER FLOW

the Mach lines, η, and the pressure, P, is given by the expression

$$d\eta = \frac{(\frac{V}{c} + \frac{dc}{dP})dP}{(f_i^2 + 2\omega_i - 2\omega - c^2)^{1/2}} \tag{1}$$

c and V designate the sound velocity and the specific volume, while ω is the specific enthalpy, defined by

$$\omega = \int VdP \tag{2}$$

ω_i is the specific enthalpy of the flow f_i at the beginning of the expansion.

Substitution of numerical values from the Appendix permits analytic integration of differential equation (1) over the pressure range of interest. For a complete expansion to zero pressure, the integral

$$\eta = \int_{P=P_i}^{P=0} d\eta = \Big[(1-9.046 \times 10^{-2}N-1.048 \times 10^{-6}P)(N-2.318 \times 10^{-5}P)^{1/2}\Big]_{P=P_i}^{P=0} \tag{3}$$

is obtained, in which P, the pressure in psi, is evaluated between the limits P_i, (the pressure of the flow f_i), and 0. N is a function of the flow f_i into the corner and is given by

$$N = \frac{f_i^2}{c_o^2} - 1 + 6.282 \times 10^{-6}P_i \geq 2.318 \times 10^{-5}P_i \tag{4}$$

The equality sign on the right hand side refers to sonic entry into the corner. In the latter case,

$$\eta \approx 0.276\ P_i^{1/2} \tag{5}$$

for moderate pressures.

As a first approximation, the change in angle η corresponding to an expansion from P_i to any pressure P in equation (3) is proportional to the square root of the pressure change. As a result, the pressure change in the expansion wedge as a function of the angle approximates a second order parabolic decay

$$P = P_i\left[1-\left(\frac{\Delta\eta}{\eta}\right)^2\right] \tag{6}$$

In all practical cases, the shockwave to be considered is spherical. Some general considerations applicable to this case are in order here. Because of the curvature of the front, the angle θ, the pressure, and consequently all other variables change with time or distance from the charge center; a stationary flow can therefore no longer be realized. However, over a very small area close to the free surface, the curvature of the front is negligible, and the stationary flow pattern illustrated in Figure 1 is applicable <u>at any one time</u> (a quasi-stationary flow). If the region of interest extends an appreciable distance down from the surface, the shock front and the expansion wedge become arcs (the latter only as an approximation). Superposition of a radial flow, parallel to the surface at the surface, as illustrated in Figure 3, makes the entire shock front and the expansion wedge at the surface quasi-stationary. The expansion wedge farther down, however, will not be completely quasi-stationary. The greater the

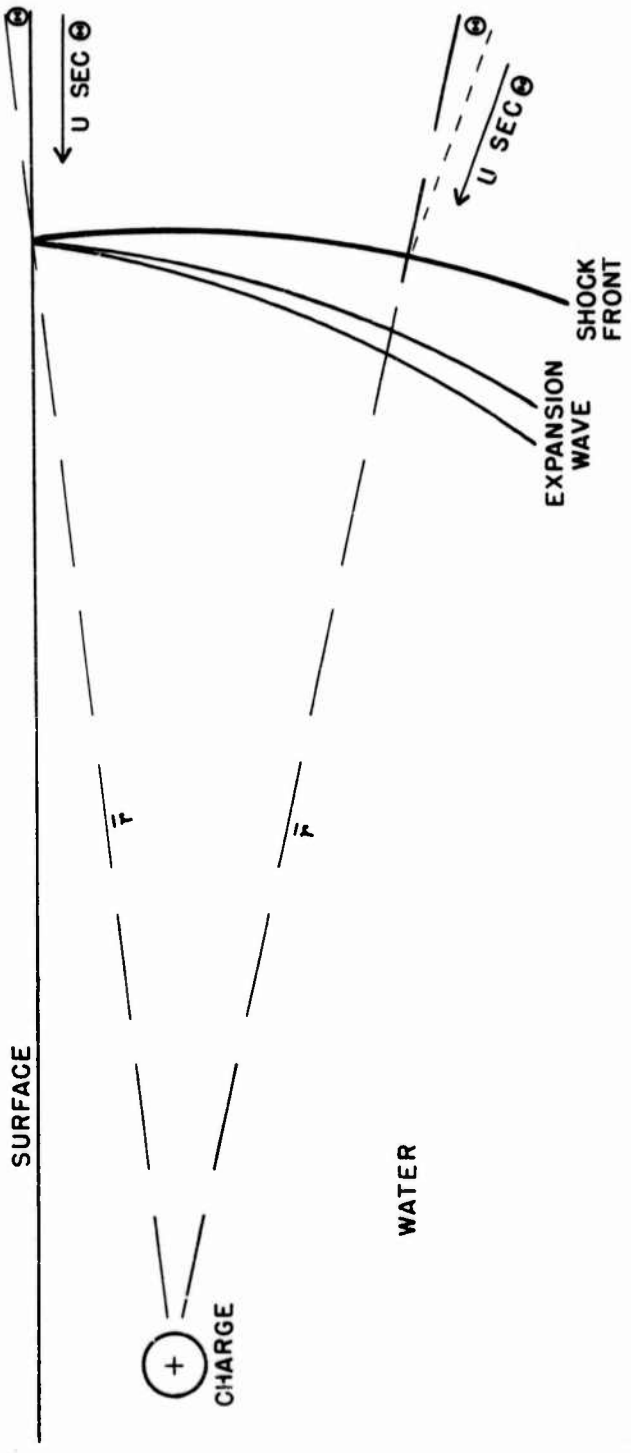

FIG. 3 REGULAR REFLECTION OF SPHERICAL SHOCKWAVE

curvature of the arcs and the greater the distance between the shock front and the expansion wave, the greater will be the deviation from the quasi-stationary flow. For the geometries considered in this paper, the deviation is not serious and can be neglected. Thus, it becomes possible here to consider a stationary flow pattern even in the case of a spherical shock-wave. This makes it feasible to extend many of the results obtained in the plane case to the actual spherical problem by an analogy to the method of images used in acoustics.

III THE CRITICAL CONDITIONS AND THE BOUNDARY OF THE ANOMALOUS REGION

For a plane shock wave, as shown in Figure 1, the flow f_i into the expansion wedge is a function of the glancing angle Θ and the pressure P. This is true because the propagation velocity U and the particle velocity u depend only on P. If for a shockwave of given pressure, the angle Θ is decreased, the absolute magnitude of f_i decreases, and eventually f_i may become sonic. In that case, the initial Mach line of the expansion wedge must be perpendicular to the flow f_i; the flow out of the wedge remains supersonic. If the flow f_i becomes subsonic, the entire Prandtl-Meyer treatment collapses, and such centered expansion at a corner is no longer possible.

The point where the flow f_i is sonic constitutes the boundary between regular and "anomalous" surface reflection. For the case of an infinite plane shockwave, the condition of a sonic flow f_i leads to a relation between the shock pressure P and the critical glancing angle Θ_{crit}: From the velocity triangle in Figure 1, it follows that

$$(U \sec\Theta - u \cos\Theta)^2 - u^2 \sin^2\Theta = f_i^2 \ . \qquad (7)$$

But f_i = c (the local sound velocity) is the condition of sonic flow; therefore,

$$(U \sec\Theta_{crit} - u \cos\Theta_{crit})^2 - u^2 \sin^2\Theta_{crit} = c^2 \qquad (8)$$

$$\text{or } \Theta_{crit} = \tan^{-1}\left\{\frac{1}{U}[c^2-(U-u)^2]^{1/2}\right\} \qquad (9)$$

where U, u, and c are functions of the shock pressure P.

The fact that the first Mach line of the expansion is perpendicular to the sonic flow f_i, leads to the expression

$$\lambda_{crit} = \sin^{-1}\left\{\frac{u}{c} \sin\Theta_{crit}\right\} \qquad (10)$$

where λ is the angle which the first expansion Mach line makes with the perpendicular to the free surface. This angle becomes very small for pressures less than 10,000 psi and can usually be neglected. In other words, the first Mach line can be considered as being perpendicular to the free surface.

If the plane shockwave of the preceding discussion is considered to be a small section of a spherical shockwave at the free water surface, the pressure P and its functions U, u, and c become functions of the radial distance from the charge center. Substitution of the numerical values given in the Appendix transforms equation (9) into

$$\tan\Theta_{crit} = \left[\frac{1.197 \times 10^{-5} P}{1+5.367 \times 10^{-6} P}\right]^{1/2} \qquad (11)$$

$$\text{and} \quad \tan \theta_{crit} = 1.820\, \bar{r}^{-.60} - 1.353\, \bar{r}^{-1.80} \quad \text{Pentolite}$$
$$= 1.574\, \bar{r}^{-.565} - .8736\, \bar{r}^{-1.695} \quad \text{TNT} \qquad (12)$$

where $\bar{r}$ represents the radial distance from the charge center expressed in charge radii*.

Thus, for a spherical wave, there exists a point at the surface beyond which the reflection is anomalous. For any particular position of the charge, that is for a charge at depth $\bar{d}$ below the surface, this point will be at a definite radial distance, $\bar{r}_{crit}$, from the charge center, given by

$$\bar{r}_{crit} = \bar{d}(1.449 + .3015\, \bar{r}_{crit}^{1.20})^{1/2} \quad \text{Pentolite}$$
$$= \bar{d}(1.449 + .4047\, \bar{r}_{crit}^{1.13})^{1/2} \quad \text{TNT} \qquad (13)$$

As $\bar{d}$ increases, $\bar{r}_{crit}$ increases, and for $\bar{d} \geq 12$, expression (13) reduces to

$$\bar{r}_{crit} = .224\, \bar{d}^{2.50} \quad \text{Pentolite}$$
$$= .354\, \bar{d}^{2.30} \quad \text{TNT} \qquad (14)$$

This shows that a region of anomalous surface reflection exists for every charge depth**. The distance from the charge center to the beginning of this region at the surface, $\bar{r}_{crit}$, increases rapidly with charge depth.

---

*Throughout this paper, symbols with bars over them will represent distances expressed in charge radii.

**Of course, the numerical equations apply only as long as the shockwave pressure-distance relationships, as given in the Appendix, are valid. According to reference [C], this is true to relatively large distances.

Next, consider a plane shockwave which suddenly interacts with the free surface at a glancing angle which is less than the critical angle. From the point of intersection of the shock front with the surface, a signal will originate which propagates with the local sound velocity c into the local particle stream of velocity u. Since the glancing angle is less than the critical angle, the horizontal velocity component of the signal is greater than that of the shock front. Thus, the surface signal overtakes the shock front. This is illustrated in Figure 4.

The path of descent of the primary surface signal must be the line along which the shockwave has the same velocity as the surface signal. This is the case where vector addition of c and u equals U, or in other words where c equals f_i. This condition is analogous to the critical condition at the free water surface, so that the path of descent may be considered a free surface, which the incident shock intersects at the glancing angle Θ_{crit}. The shock front below this path is unaffected by the surface signal, above this path it is attenuated. The region where the shock front is attenuated constitutes the "anomalous" region.

According to these considerations, Keil [I] has defined the boundary of the anomalous region as the curve which intersects the radius vector $\bar{r}$ from the charge center at the critical angle. This leads to a differential equation for the rate of descent of the boundary:

$$\frac{d\bar{y}_{crit}}{d\bar{r}} = \tan \Theta_{crit}\left[1 - \left(\frac{\bar{d}-\bar{y}_{crit}}{\bar{r}}\right)^2\right]^{1/2} - \frac{\bar{d}-\bar{y}_{crit}}{\bar{r}} \qquad (15)$$

where $\bar{y}_{crit}$, expressed in charge radii, is the depth of the anomalous region boundary beneath the free surface. For a

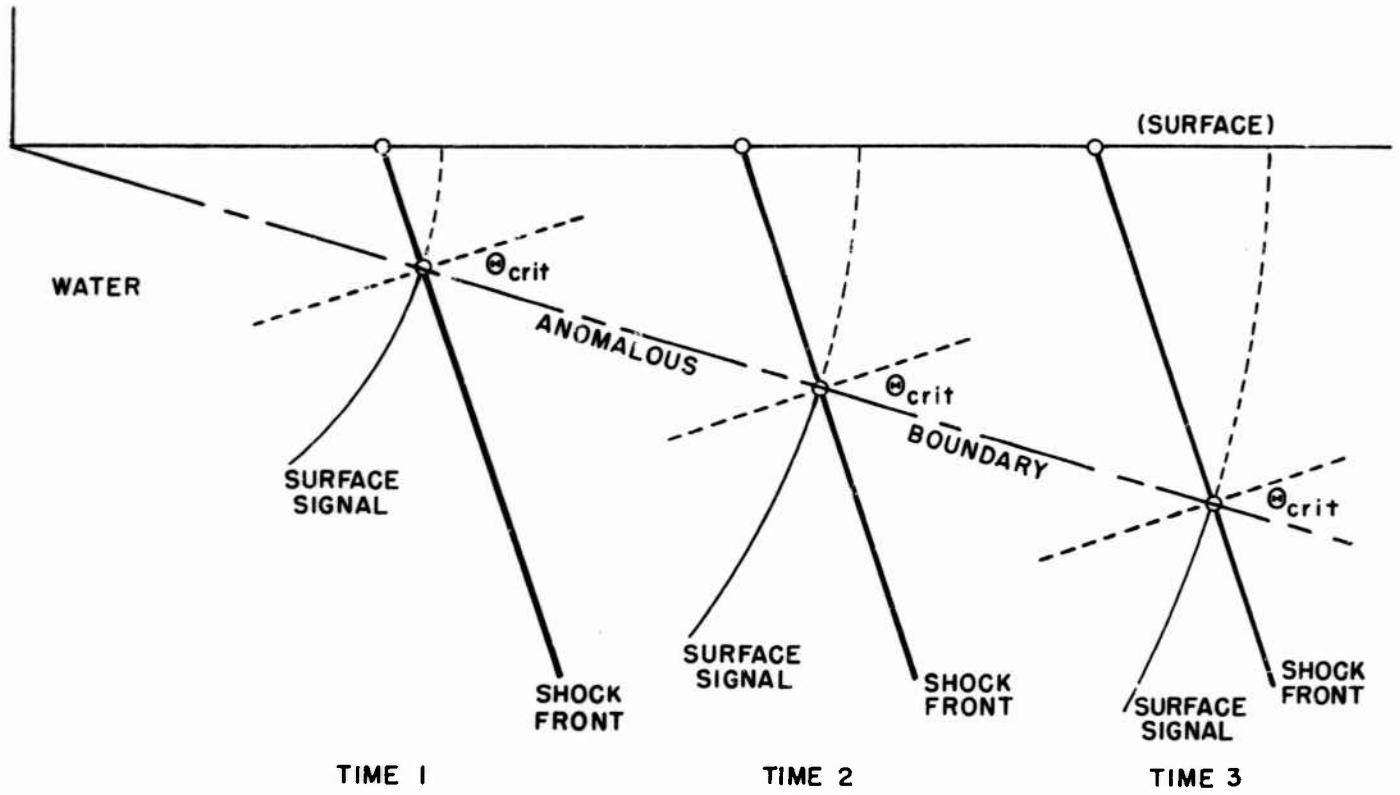

FIG. 4 PROPAGATION OF PRIMARY SIGNAL ALONG PLANE SHOCK FRONT
(RESTING POINT OF OBSERVATION)

spherical wave, the critical angle is a function of the radius vector $\bar{r}$, as shown in equation (12). Substitution of the appropriate expressions in the differential equation (15) and integration* lead to the expressions

$$\frac{\bar{d}-\bar{y}_{crit}}{\bar{r}} = \sin\left(3.033\ \bar{r}^{-.60} - .752\ \bar{r}^{-1.80} + .497\ \bar{r}^{-3.00} - k'\right) \quad \text{Pentolite}$$

$$= \sin\left(2.784\ \bar{r}^{-.565} - .515\ \bar{r}^{-1.695} + .257\ \bar{r}^{-2.825} - k'\right) \quad \text{TNT} \qquad (16)$$

k' is a constant of integration evaluated at the point of critical surface reflection; that is, at $\bar{r} = \bar{r}_{crit}$, $\bar{y}_{crit}$ must be 0.

In the preceding derivation, the path of a signal originating at the point of critical surface reflection was traced. It appears reasonable that this signal is indeed the first to arrive at the shock front at a given depth y; however, no proof is yet at hand that a signal originating at the surface prior to the point of critical reflection must arrive at the shock front at a later time.

IV THE ANOMALOUS REGION

The discussions of the previous section lead to a definite picture of the shockwave in the anomalous region: a spherical shock front invades the undisturbed water. An expansion wave originating from the free surface has overtaken the incident shock front near the surface, and its head intersects the shock front at the known depth $\bar{y}_{crit}$. The shock is attenuated when overtaken by this rarefaction wave. The shock

*W. Mostow, in a private communication, pointed out that the differential equation (15), due to Keil [I], can be integrated analytically.

pressure will decrease from the free water value at $\bar{y}_{crit}$ to a value P_s at the surface, in a manner depending on the pressure profile of the rarefaction wave.

At this point the assumption is made that the conditions in and immediately below the anomalous region can be represented approximately by a quasi-stationary flow pattern together with a nonstationary rarefaction wave. Figure 5 illustrates such a flow pattern for a plane shockwave. A flow, $-U_F \sec \Theta$, which makes the undistorted shock front stationary, is superposed. The head of the nonstationary rarefaction wave intersects the shock front at the boundary of the anomalous region, that is, at the depth $\bar{y}_{crit}$. The point of intersection of the actual shock front with the surface must coincide with the stationary rear of the nonstationary rarefaction wave. The remaining pressure must be released at this point; this is accomplished by a stationary centered expansion wave, the Prandtl-Meyer corner flow.

The pressure P_s at the rear of the nonstationary rarefaction wave can be found from the condition that the flow should be stationary there. This leads to the following procedure: The flow into the nonstationary wave is split into components parallel and perpendicular tc the wave.

Parallel component $\cong$

$$(U_F \sec\Theta - u_F \cos\Theta) \sin\gamma - u_F \sin\Theta \cos\gamma \qquad (17)$$

Perpendicular component $\cong$

$$(U_F \sec\Theta - u_F \cos\Theta) \cos\gamma \qquad (18)$$

where $\gamma = (\Theta_{crit} - \Theta)$. The wave accelerates the perpendicular

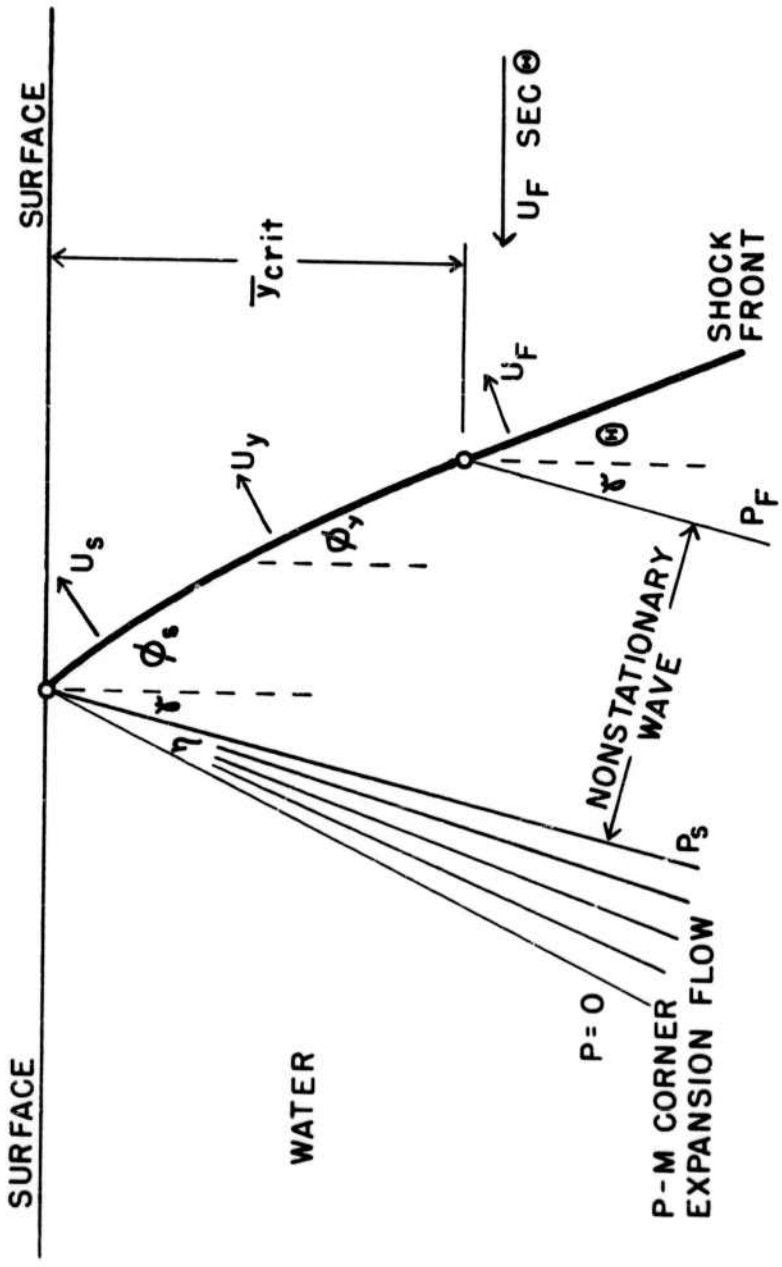

FIG. 5 STATIONARY FLOW PATTERN IN ANOMALOUS REGION

component of the flow. For a plane wave, the acceleration depends only on the overall pressure change. At the rear of the wave, the perpendicular component of the flow must be equal to the local sound velocity. Thus,

$$c_s = (U_F \sec\Theta - u_F \cos\Theta) \cos\gamma + \int_{P_s}^{P_F} \frac{V}{c}\, dP \qquad (19)$$

The last term, the Riemann function, represents the velocity increment which the nonstationary wave imparts to the flow. The expression can be solved for the pressure P_s at the beginning of the stationary expansion centered at the surface.

Actually, the shock front in the anomalous region is bent back and, because of its lower peak pressure there, propagates at a lower velocity than the unattenuated shock. As a rough approximation, it can be assumed that these two effects cancel as far as the horizontal propagation velocity of the wave is concerned. In other words,

$$U_F \sec\Theta = U_y \sec\phi_y = U_s \sec\phi_s \qquad (20)$$

where ϕ represents the glancing angle of the attenuated front, and the subscripts s and y refer to the surface and to any depth y in the anomalous region respectively (see Figure 5). Equation (20) states that the superposed flow $U_F \sec\Theta$ makes the entire shock front stationary with respect to the surface. Substitution of the numerical values from the Appendix into this equation leads directly to a relation between ϕ_y and P_y, the peak shock pressure at any depth y:

$$P_y = 1.863 \times 10^5 \left[\frac{(1 + 5.367 \times 10^{-6} P_F) \cos\phi_y}{\cos\Theta} - 1 \right]. \qquad (21)$$

It can be shown that rotation is introduced into a stream on passing through a bent shockwave [0]. In the present case, this effect causes the rarefaction wave to bend back slightly close to the surface. At the relatively low pressure of interest here, this bending is small and can be neglected.

Next, equation (19) is evaluated for the quasi-stationary case of a plane wave, whose parameters change with distance from the origin like those of a spherical shockwave. This leads to the expression

$$\begin{aligned} P_s &= 1.570 \times 10^5\, \bar{d}\bar{r}^{-1.60} - 8.63 \times 10^3\, \bar{r}^{-1.20} \quad \text{Pentolite} \\ &= 1.360 \times 10^5\, \bar{d}\bar{r}^{-1.565} - 3.80 \times 10^3\, \bar{r}^{-1.13} \quad \text{TNT} \end{aligned} \tag{22}$$

For the actual spherical case, an analogy to the method of images permits arcs to be substituted for the plane wave configuration in Figure 5. Account must be taken of the spherical divergence term arising from the equation of continuity. This term, which must appear on the right hand side of equation (19), is approximated by

$$\frac{1}{\rho_o c_o \bar{r}} \int_o^{\bar{x}_{total}} P \, d\bar{x} \quad (\bar{r} \gg \bar{x}_{total}) \tag{23}$$

where $\bar{x}$ is the distance from the back of the nonstationary wave perpendicular to its direction of propagation, $\bar{x}_{total}$ is its total width and ρ_o is the density of the undisturbed water. (23) is conveniently expressed as a correction term

$$\Delta P_{spherical} = \frac{q\, \bar{x}_{total}\, P_F}{\bar{r}} \tag{24}$$

which must be added to the incident surface pressure of the

plane case, equation (22). The symbol q in equation (24) represents a fraction, which depends on the pressure profile of the rarefaction wave. Its value, based on experimental observations, appears to be approximately .85.

The pressure profile of the rarefaction wave is related by a geometric argument to the pressure-depth variation along the shock front in the anomalous region. The latter is related to the angle ϕ_y of the shock front in the anomalous region by the stationary flow assumption and the Rankine-Hugoniot conditions [see equation (21)]. From various qualitative arguments, the pressure, and therefore also the angle ϕ_y, is expected to change most rapidly with depth near the surface and most slowly at the lower edge of the anomalous region. This suggests a power law for the angle ϕ_y as given by the expression

$$\phi_y = (\phi_s - \theta)(1 - \tilde{y})^n + \theta \tag{25}$$

where $\tilde{y} = \bar{y}/\bar{y}_{crit}$ is the "relative depth" in the anomalous region, and n is a constant, whose value from actual experiments appears to be approximately 4.

Knowledge of the angle ϕ_y as a function of depth permits a rough estimate of the total lag of the actual shock front at the surface behind one which is not attenuated by surface signals. This is given by the following equation for the plane wave case:

$$\bar{L}_{total} = \int_o^{\bar{y}_{crit}} \tan \phi_y \, d\bar{y} - \bar{y}_{crit} \tan\theta \tag{26}$$

which becomes

$$\bar{L}_{total} = \frac{\bar{y}_{crit} \tan \Phi}{(n + 1)} \tag{27}$$

when $\Phi = (\phi_s - \theta)$ is relatively small. The lag at the surface behind that at any depth y in the anomalous region is similarly

given by

$$\bar{L}_y = \frac{\bar{y}_{crit} \tan\Phi}{(n+1)} [1 - (1-\tilde{y})^{n+1}] \quad . \tag{28}$$

These equations, which were derived for plane waves, are also approximately correct for the spherical case.

The pressure of the nonstationary rarefaction wave is constant along a line for which $\bar{x}$, defined in connection with equation (23), is constant. Thus, the pressure profile of the rarefaction wave follows from the profile of the shock front in the anomalous region [given by equations (21) and (25) as discussed previously] if the corresponding values of $\bar{x}$ and $\bar{y}$ along the shock front are known. This relation between $\bar{x}$ and $\bar{y}$ follows from geometric considerations and is given by the approximate expression

$$\tilde{x} \approx \frac{\frac{\tan\Phi}{n+1}[1-(1-\tilde{y})^{n+1}] + \tilde{y}\left[\frac{\bar{d}+\bar{y}_{crit}}{\bar{r}} + \sin\gamma\right] - \tilde{y}^2 \frac{\bar{y}_{crit}}{2\bar{r}}}{\frac{\tan\Phi}{n+1} + \frac{\bar{d}+\bar{y}_{crit}}{\bar{r}} + \sin\gamma - \frac{\bar{y}_{crit}}{2\bar{r}}} \tag{29}$$

where $\tilde{x} = \bar{x}/\bar{x}_{total}$ measures the relative distance through the nonstationary wave. Note that $\tilde{x} = 0$ at the stationary end of the wave, and $\tilde{x} = 1$ at the head of the wave.

The flow through a stationary expansion wave was solved for the plane case in Section II of this report. Thus, in equation (3), P_s must be substituted for P_i, and the total velocity of the flow into the wedge is given by

$$\frac{f_i^2}{c_o^2} \approx \left\{(1 + 8.449 \times 10^{-6} P_s)^2 + \left[\frac{(1+2.463 \times 10^{-6} P_F)\sin\gamma}{\cos\Theta}\right]^2\right\} \tag{30}$$

This provides everything to calculate the total deflection η

of the Mach lines at the Prandtl-Meyer corner. From this and from the definition of γ, stated in conjunction with equations (17) and (18), it follows that ψ, the angle which the rear of the Prandtl-Meyer expansion wedge makes with the perpendicular with the surface, is given by

$$\psi = \gamma + \eta \tag{31}$$

It appears worthwhile here to make a few remarks on the assumption of stationary flow, which was introduced in this section. Actually, the plane wave case consists of a plane incident shock front and an approximately cylindrical expansion wave, which is attenuating the incident shock. The attenuated part of the shock front is traveling at a slower rate than the unaffected part and thus eventually bends back near the surface. Strictly speaking, it is only possible to make the unattenuated part of the shock front stationary at any one time; however, the theory derived in this section assumes a stationary flow through the entire shockwave configuration. The approximate character of this treatment shows up in nonstationary effects at the surface: the superposed flow through the nonstationary rarefaction wave is not quite perpendicular to the wave front. The flow through the stationary rear of this wave is thus slightly greater than sonic, a condition which tends to increase the incident pressure at the surface point.

V THE CONSTRUCTION OF PRESSURE-TIME HISTORIES

If the theory developed in the preceding sections is to be of practical significance, it must predict satisfactorily the pressure-time history of a shockwave at a distance r from the charge center and at a depth y below the free surface. A procedure which yields approximate pressure-time histories is outlined in this section.

To begin with, the quantities $\bar{r}$, $\bar{d}$, θ, θ_{crit}, $\bar{y}_{crit}$, P_F, and P_s for the plane case are calculated from the known charge weight and geometry of the problem by means of the appropriate equations in the text. A scaled diagram of the shock front is then drawn, the bending back effect near the surface being neglected at first. At the critical depth, $\bar{y}_{crit}$, on the shock front, a line is drawn which makes the angle θ_{crit} with the radius vector $\bar{r}$ from the charge center. The line is extended back until it intersects above the free surface a line passing through the charge center and perpendicular to the surface. The point of intersection, A in Figure 6, which in a sense represents an "image" point for the nonstationary

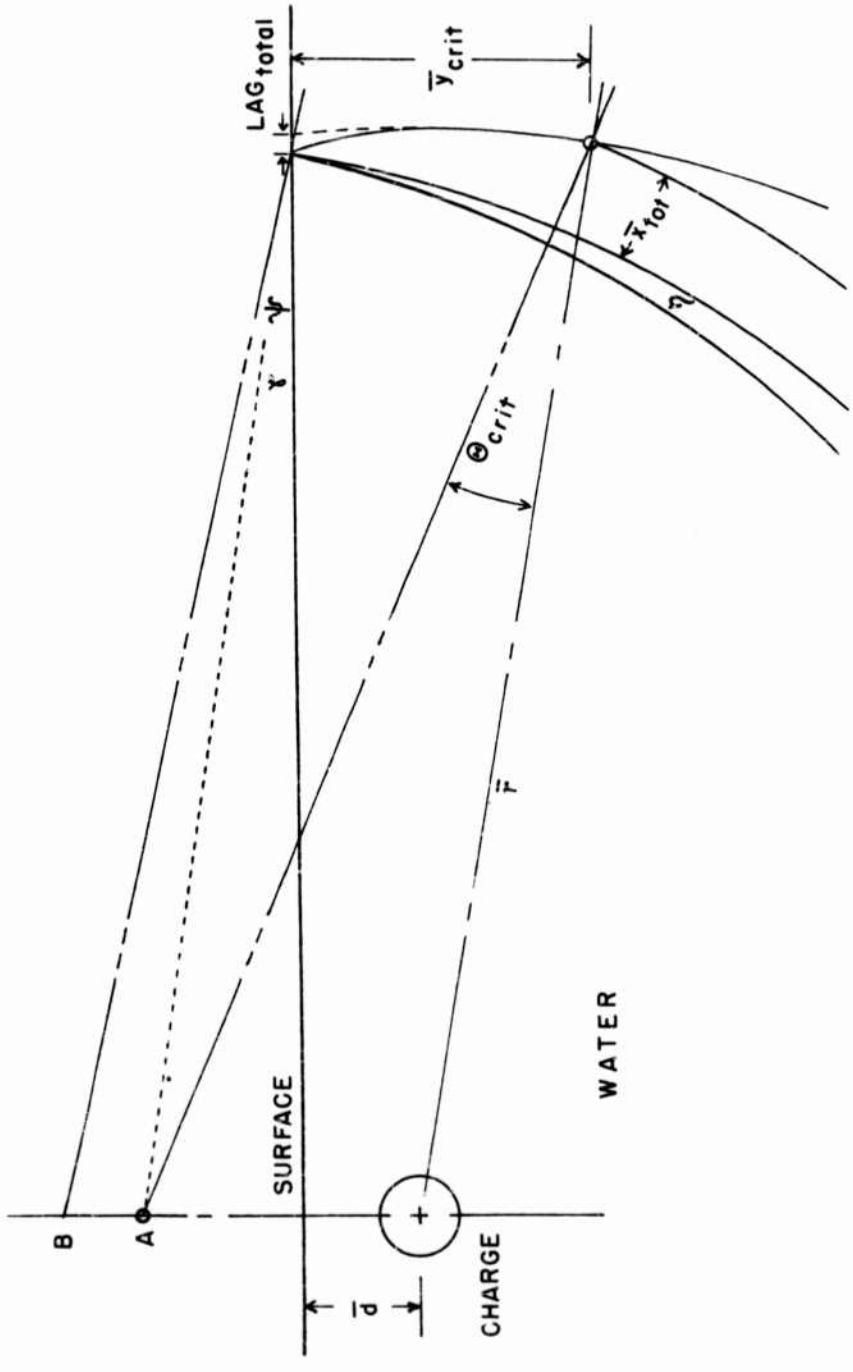

FIG. 6 APPROXIMATE CONFIGURATION OF SPHERICAL WAVE WITH ANOMALOUS SURFACE CUT-OFF

rarefaction wave, serves as a center for two concentric circles passing through the critical point on the shock front and through the surface point of the shock front respectively. The distance between these circles represents a first approximation to the width, $\bar{x}_{total}$, of the nonstationary wave. It is now possible to calculate $\Delta P_{spherical}$ and P_s for the spherical case, and hence also ϕ_s, ϕ_y, Φ, and $\bar{L}_{total}$. If the latter quantity is appreciable, it must be included in $\bar{x}_{total}$, and values for P_s, ϕ_s, etc., may have to be recalculated. Finally, ψ is calculated, and the corresponding "image" point, B in Figure 5, is found by drawing a line through the corrected surface point of the incident shock, which makes the angle ψ with the free surface. The point of intersection of this line with the perpendicular to the surface above the charge serves as the center of a circular arc representing the end of the centered expansion. The final diagram is as indicated in Figure 6.

Next, a path through the shockwave configuration is considered which corresponds approximately to the way the shockwave passes a gauge. All distances are then converted to a time scale. It is sufficient to use the sound velocity in undisturbed water for this purpose. The peak shock pressure and the pressure decay due to the nonstationary and the stationary centered wave are calculated from the appropriate equations in the text. The results are superposed on the pressure-time decay curve of the free water shockwave as given in equation (A4) of the Appendix, and the resulting curves are smoothed out. The approximate pressure-time histories thus drawn represent the results obtainable with the present theory.

In conclusion, it may be worthwhile to discuss the range of applicability of the present work. In general, it is possible to calculate pressure-time histories for charge

depths of 3 charge radii or more, at distances where the free water shockwave peak pressure is 10,000 psi or less. In this case, the equations are all in analytical form, and agreement with experiment* appears satisfactory. It should be noted that the present theory was derived for the ideal case of a semi-infinite homogeneous medium and a perfectly plane free boundary. However, under actual experimental conditions, other factors enter - such as surface roughness, temperature and density gradients in the undisturbed medium [G], the presence of a solid bottom, etc. Their effects depend on the size and locale of the particular explosion and must be investigated separately. Finally, it should be pointed out that the present results do not apply to charge depths of less than 2 charge radii. Here the assumptions of the theory are no longer satisfactory, and in addition, the very difficult problem of an air-backed explosion arises. It is felt that for these very shallow charge depths, more work, especially experimental, is necessary.

* See References [E] and [Q].

APPENDIX

FREE WATER SHOCKWAVE PARAMETERS

For a shock front moving through a fluid medium, the hydrodynamic and thermodynamic transitions are specified by the Rankine-Hugoniot relations; for an expansion wave, on the other hand, isentropic changes are applicable. If the initial state of the medium is known, and if sufficient P-V-T data is available, both cases can be expressed completely in terms of one independent variable - for example the pressure change. For the relatively low pressure changes applicable to this report, the isentropic and the Hugoniot curves for water are almost identical and differ but little from the isothermal.

The following Rankine-Hugoniot parameters for fresh water, initially at rest and at 20°C and 1 atm., have been calculated with the aid of references [A,H,J] and are quite satisfactory up to pressures of 30,000 psi. For much higher pressures, the numerical values given in reference [P] should be used. The following relations hold for this low pressure region:

$$\begin{aligned} U &= c_o(1 + 5.367 \times 10^{-6}\ P) \\ u &= c_o(2.89 \times 10^{-6}\ P) \\ U - u &= c_o(1 + 2.463 \times 10^{-6}\ P) \\ c &= c_o(1 + 8.449 \times 10^{-6}\ P) \end{aligned} \qquad \text{(A1)}$$

where P is the excess pressure in psi, U is the propagation velocity of the shockwave, and u and c are the particle velocity and local sound velocity behind the shock front. c_o, the sound velocity in the undisturbed water (20°C and 1 atm.), is 1483 meters/second.

An equation of state for water, applicable to the true as well as the Hugoniot adiabatic up to a pressure of 30,000

psi, is given by the expression

$$V = 1.00177\ (1-3.04 \times 10^{-6}P + 2.3 \times 10^{-11}P^2) \qquad (A2)$$

where V is the specific volume of the water, and an initial state of 20°C and 1 atm. is assumed.

The experimental free water shockwave peak pressure data are conveniently expressed in terms of the initial charge radius For pressures below 30,000 psi

$$P_F = 2.77 \times 10^5\ \bar{r}^{-1.20} \quad \text{Pentolite, } \rho = 1.63 \text{ gm/cc [F]}$$
$$P_F = 2.07 \times 10^5\ \bar{r}^{-1.13} \quad \text{TNT, } \rho = 1.55 \text{ gm/cc [D]} \qquad (A3)$$

where P_F is the free water peak pressure in psi, $\bar{r}$ is the radial distance from the center of the charge expressed in charge radii, and ρ is the loading density.

The free water pressure decay behind the shock front, observed at a fixed point, is given by the expression

$$P = P_F e^{-t/\theta} \qquad P_F \leq 15{,}000 \text{ psi}$$

where

$$\theta = 31.1\ W^{1/3}\ \bar{r}^{.23} \quad \text{Pentolite, } \rho = 1.63 \text{ gm/cc [F]} \qquad (A4)$$
$$\theta = 41.9\ W^{1/3}\ \bar{r}^{.18} \quad \text{TNT, } \rho = 1.55 \text{ gm/cc [D]}$$

Here P is in the same units as P_F, t is the time after shock front arrival in microseconds, θ is the time constant in microseconds, and W is the charge weight in lbs. This formula is valid only up to $t \approx \theta$.

REFERENCES

[A] Amagat, E. H., Ann. de chim. et phys. (6), 29, 68-136, 505-574 (1893), as quoted by Dorsey, N.E., "Properties of Ordinary Water Substance", American Chemical Society Monograph Series No. 81, Reinhold Publishing Co., New York, 1940, pages 207-211.

[C] Arons, A. B. and Yennie, D. R., "Long Range Shock Propagation in Underwater Explosion Phenomena I", NAVORD Report 424 (1949)

[D] Coles, J.S., et al., "Shock Wave Parameters from Spherical HBX and TNT Charges Detonated under Water", NAVORD Report 103-46 (1946)

[E] Coles, J.S., et al., "Measurement of Underwater Explosions near the Surface and Bottom of the Ocean", NAVORD Report 105-46 (1947)

[F] Cole, R. H., "Underwater Explosions", Princeton University Press,1948. Page 242.

[G] Herring, C., "The Physics of Sound in the Sea", Summary Technical Report of Division 6, NDRC, Volume 8, Washington, D.C. (1946),Chapter 9, as well as references listed therein.

[H] Holton, G., "Ultrasonic Propagation in Liquids Under High Pressures: Velocity Measurements on Water", Journal of Applied Physics 22, 1407-13 (1951)

[I] Keil, A. H., "Boundary of Disturbance for Non-Linear Reflection of Underwater Shock Waves at a Free Surface", UERU Report 3-48 (1948)

[J] Kirkwood, J. G. and Montroll, E. W., "The Pressure Wave Produced by an Underwater Explosion III", OSRD No. 813 (1942)

[L] Meyer, Th., "Ueber zweidimensionale Bewegungsvorgaenge in einem Gas, das mit Ueberschallgeschwindigkeit stroemt". Dissertation, Goettingen, 1908, as reprinted in "Foundations of High Speed Aerodynamics", Dover, New York, 1951.

[O] Sauer, R., "Theoretische Einfuehrung in die Gasdynamik", Springer, Berlin, 1943, Paragraphs 19 and 20.

[P] Snay, H. G. and Rosenbaum, J. H., "Shockwave Parameters in Fresh Water for Pressures up to 95 Kilobars", NAVORD Report 2383 (1952) as well as other references quoted therein.

[Q] Sokol, G. M., "The Reflection of Small Charge Shock Waves from a Free Surface", NAVORD Report 410 (1947).

NAVORD Report 2710

DISTRIBUTION LIST

		Copies
Chief, Bureau of Ordnance	Attn: Ad3	2
	Attn: Ad6	1
	Attn: Re06	1
Armed Services Technical Information Agency, Document Service Center, Knott Building, Dayton 2, Ohio		5
Prof. Arnold B. Arons, Physics Department, Amherst College, Amherst, Mass.		1
Dr. Joseph H. Rosenbaum, Box 3323, Bellaire, Texas		1
Dr. A.H.Keil, Code 270, Norfolk Naval Shipyard, Portsmouth, Virginia		1
Brown University, Providence, Rhode Island		
Attn: Division of Applied Mathematics		1
Prof. Harold Wayland, California Institute of Technology Pasadena 4, California		1
University of California, Berkely 4, California		
Attn: Prof. J. W. Johnson (Fluid Mechanics Laboratory)		1
Attn: H. A. Schade (Dir. of Engineering Research)		1
University of California, Scripps Institute of Oceanography, La Jolla, California,		
Attn: Dr. R. R. Revelle, Director		1
Harvard University, Cambridge 38, Massachusetts		
Attn: Prof. George F. Carrier (Dept. of Engineering Sciences)		1
Attn: Prof. G. Birkhoff (Dept. of Mathematics)		1
Armour Research Foundation, 35 W. 33rd Street, Chicago 16, Illinois	Attn: Dr. F. Porzel	1
	Attn: Dr. S. J. Fraenkel	1
Columbia University, Department of Civil Engineering and Engineering Mechanics, New York 27, N. Y.		
Attn: Dr. H. H. Bleich		1
Attn: Dr. R. Skalak		1
Indiana University, Department of Mathematics Bloomington, Indiana, Attn: Prof. D. Gilbarg		1

DISTRIBUTION LIST (Cont'd.)

	Copies
State University of Iowa, Iowa Institute of Hydraulic Research, Iowa City, Iowa, Attn: Dr. L. Landweber	1
University of Maryland, Institute for Applied Mathematics and Fluid Dynamics, College Park, Maryland Attn: Dr. Elliott W. Montroll	1
New York University , Institute of Mathematical Sciences, 25 Waverly Place, New York 3, N. Y. Attn: Dr. R. Courant	1
Director Woods Hole Oceanographic Institution Woods Hole, Massachusetts	1
Ramo-Wooldridge Corporation Los Angeles, California Attn: Dr. J. Richardson	1
University of Texas, Defense Research Laboratory Austin, Texas Attn: Dr. Otto Hill	1